

during night and spawning is in water, floating on edges as colloid egg-mass (211–232 tablets) held with strong adhesive force. Eggs are long oval (0.2 mm long, 0.08 mm wide) and yellow. Single egg-mass may take 4–8 days to complete hatching. The hatched-out larvae are not immediately free, but cluster to egg-mass and feed on gum, rapidly increasing the body size by almost 2.5 times. Later they migrate to floating leaf surface and penetrate through a circular hole of about 0.2 mm.

The larvae are yellowish-brown and grow to 10–11 mm length (Figure 1c); brown head with black mouthparts, serrated big jaws, five antennae and gradually reducing to get embedded in the chest after thoracic clemency. Abdomen is cylindrical with two pairs of finger-anal gill units on posterior end. Mature larvae break the epidermis and move to the front of the floating upper surface of the leaf for pupation. Pupation starts within 14–17 days after mining into the leaf and feeding. Pupa is 4–6 mm long, light green in silky cocoon and the pupal period varies from 3 to 7 days.

Earlier reports show that leaf miners such as *Liriomyza congesta* (Becker), *Melanagromyza cunctans* (Meigen), *Phytomyza horticola* (Goureau) (Diptera: Agromyzidae) and gallmidges such as *Asphondylia melanopus* (Kieffer), *Contarinia barbichei* (Kieffer), *C. loti* (De Geer), *C. medicaginis* (Kieffer), *Dasi-neura loti* (Kieffer) and *Jaapiella loticola* (Rubsamen) attack lotus during different stages of development^{8,9}. But none of these symptoms and damage exactly coincide with those developed by *S. nelumbus*. India in the past has witnessed continuous species invasions leading to severe imbalance to crop and human ecosystems³. With shrinking barriers in the era of globalization, the chances of invasion are burgeoning, even after strict

quarantine enforcements¹⁹. Recent invaders in the Indian ecosystems such as *Erythrina* gall wasp (*Quadraslichus erythrinae* Kim)²⁰, spiraling whitefly (*Aleurodicus disperses* Russell)²¹ and coconut mite (*Aceria guerreronis* Kieffer)²² speak of alarming proliferation facilitated by the absence of natural enemies. No immediate trade barrier to India needs to be considered as far as the cultivation is domestic market-oriented, infestation remains localized and no alternate hosts are reported. However, quarantine procedures have to be reinforced when it comes to the international exchange of lotus material. Managing *S. nelumbus* invites special challenges since any chemical pesticide in the freshwater in such a wide area could be an ecological far-reaching disaster. Environment-friendly practice of draining the commercial fields during the peak infestation to destroy the egg-masses is not applicable to these low-lying 'Kole' lands. Our experiments with neem oil-soap emulsion spray at fortnightly intervals during the peak winter months have shown a reduction in severity by 63%. Concentrations beyond 1% were supra optimal.

1. United States Department of Agriculture, *Fed. Regist.*, 1999, **64**, 6163–6166.
2. Mondor, E. B., Tremblay, M. N. and Messing, R. H., *Biol. Inv.*, 2007, **9**, 87–100.
3. Mathew, D. and Duraimurugan, P., *Plant Prot. Bull.*, 2002, **54**, 25–34.
4. The National Invasive Species Council, Paper submitted by Invasive Species Advisory Committee, ISAC, 2006, pp. 1–11; www.invasivespeciesinfo.gov/docs/council/isacdef.pdf, retrieved on 18 July 2007.
5. Moyle, P. B. and Light, T., *Biol. Conserv.*, 1996, **78**, 149–161.
6. Lee, C. E. and Bell, M. A., *Trends Ecol. Evol.*, 1999, **14**, 284–288.
7. Goel, A., Sharma, S. C. and Sharga, A. N., *Bot. Gardens Conserv. Int.*, 2001, **3**, 1–5.

8. Jones, D. A. and Turkington, R., *J. Ecol.*, 1986, **74**, 1185–1212.
9. European and Mediterranean Plant Protection Organization. *EPPPO Bull.*, 2002, **32**, 407–421.
10. Alzugaray, R., *Lotus Newsl.*, 2003, **33**, 11–18.
11. Shen, B. Y., *Plant Prot.*, 1987, **13**, 37–38.
12. Gao, D., *Entomol. J. East China*, 2001, **10**, 113–116.
13. Anon., www.agridata.gov.cn/bjdrcc_web/from/detail.aspx?p_iID=669&p_iModuleID=88&ColumnID=0&Authority=0, 2006, retrieved on 25 April 2007.
14. Flower Network, www.flower.ag365.com, 2007, retrieved on 25 April 2007.
15. *Package of Practice Recommendations – Crops*, Kerala Agricultural University, 2003, 12th edn, p. 1.
16. Anon., *Deshabhimani* (Malayalam), 18 March 2007, p. 4.
17. Anon., *Deshabhimani* (Malayalam), 24 March 2007, p. 10.
18. Iqbal, K., *Chandrika* (Malayalam), 3 May 2007, p. 9.
19. Duraimurugan, P. and Mathew, D., *Plant Prot. Bull.*, 2001, **53**, 23–26.
20. Faizal, M. H., Prathapan, K. D., Anith, K. N., Mary, C. A., Lekha, M. and Rini, C. R., *Curr. Sci.*, 2006, **90**, 1061–1062.
21. Palanisamy, M. S., Pillai, K. S., Nair, P. R. and Mohandas, C., *Cassava Newsl.*, 1995, **19**, 6–7.
22. Sathiamma, B., Nair, C. P. R. and Koshy, P. K., *Indian Coconut J.*, 1998, **29**, 1–3.

Received 24 July 2007; revised accepted 8 May 2008

DEEPU MATHEW*
P. V. HABEEBURRAHMAN

Krishi Vigyan Kendra,
Kerala Agricultural University,
Tavanur 679 573, India
*For correspondence.
e-mail: deepuhort@gmail.com

Geotechnical characteristics of siliceous sediments from the Central Indian Basin

Geotechnical properties of sediments provide an insight into their behaviour when the natural state of deposition is changed due to artificial conditions. Acoustic and gamma-ray attenuation methods permit continuous recordings of physical prop-

erties with core depth. However, such studies invariably require large investment, undisturbed sediment core and ship time with geotechnical instrumentation. Although it is easy to collect data from shallow-water sediments, collection

of undisturbed deep-sea sediments is difficult. The properties are closely correlated¹, since their penetration depends upon the physico-mechanical condition of the sediment. Moreover, sediment type, shear strength and burrowing capacity of

benthic organisms are mutually inter-related. Geotechnical properties are also known to affect the distribution and abundance of benthic organisms and vertical distribution of meiobenthos². Here geotechnical characteristics of sediments from a selected area in the Central Indian Basin (CIB) are described.

The study area (10 × 10 nm at 10°S, 76°E) used for environmental assessment studies of deep-sea mining in the CIB is composed of siliceous ooze/clay, and marked with very low sedimentation rates³ of 2–2.5 mm ky⁻¹ and water depth of about 5400 m. Bathymetric profiles⁴ showed that the area has flat topography and nodule abundance of 2 kg m⁻².

A box core (50 × 50 × 50 cm) was used to collect the ten sediment cores from the study area (Figure 1) during the cruise AA *Sidorenko-61*. Acrylic tubes of 5.7 and 12 cm diameter and 50 cm length were used to collect the sediments from each box core. Samples for water content, specific gravity and grain-size analysis were collected at 2 cm interval for first 10 cm and at 5 cm thereafter, and were preserved in polythene bags at 4°C to avoid any water loss. Shear strength of the sediment was measured immediately on-board using vane shear apparatus (AIMIL, India) with rotation rate of 90° min⁻¹ and vane of 2.54 cm height and 1.2 cm diameter. Water content was calculated on dry basis after drying the sample for 24 h at 105°C and corrected for salinity⁵. Specific gravity was determined using specific gravity bottles⁶. Porosity, void ratio and wet bulk density were estimated⁷ assuming complete saturation of sediments. Sand, silt and clay percentages were calculated by standard pipette method⁸. The oriented glass slides were prepared from carbonate-free fraction (<2 µm) and air-dried. Clay minerals were identified⁹ after glycolating the glass slides at 100°C and then passing through a Philips PW 1840 X-ray diffractometer from 3° to 21° 2θ using CuKα radiation. The weight percentages of smectite, illite, kaolinite and chlorite were calculated⁹ using their peak areas from the X-ray diffractograms.

All cores have dark brown (5YR3/4) homogeneous sediments in the upper 10 cm, followed by light yellowish-brown (10YR5/4) clays with intercalation and features of bioturbation. The maximum length of the cores obtained was 41 cm.

The geotechnical properties of clay sediments are strongly influenced by the

fabric, i.e. structure, form and particle arrangement¹⁰. The sediments exhibit a wide range of specific gravity (1.81–2.43) and porosity (85.9–92.4%). The average wet bulk density of 1.15 g cm⁻³ (Table 1) is due to fine grain size, non-clay and clay minerals, and voids present. High porosity is attributed to radiolarian fossil tests and bioturbation which leads to compression of the sediments. The silty-clay sediments have high content of illite (Table 1), and show medium to high plasticity¹¹. Though smectite is a highly water-absorbing clay mineral¹², it does not show relationship with any geotechnical parameters. The high void ratio probably suggests isotropic fabric of particles in the illite-rich sediments explained by Bennett *et al.*¹³.

The X-ray analyses showed a poorly developed smectite peak but well developed illite, chlorite and kaolinite peaks in all the cores (Figure 2). It is reported¹⁴ that illite and chlorite are essentially from the Himalaya–Tibet range, through the river system, whereas kaolinite is dominantly from Australia by aeolian

and marine currents. Smectite is abundantly reworked from weathering of basalts and other continental rocks, and also from submarine volcanics. The poorly developed peaks of smectite in the present study support the earlier observation¹⁴.

Significant positive correlation (Table 2) of water content with clay ($r = 0.490$) indicates control of very fine grains on the water content. Higher silt than clay content and very low amount of sand is due to poorly sorted grains, that lead to voids in the sediment. The water content does not show significant relationship with any particular clay mineral, though smectite is known to have high water-retaining capacity. The microfabric of the sediments must have an important role as it affects the geotechnical properties, especially when siliciclastic platy particles have edge-to-face contacts with clay particles. This type of fabric gives high void ratio, high water content, and low wet bulk density¹⁵. Therefore, it is imminent that silt and clay particles in the sediments are more responsible for water content and porosity than clay mineral.

Table 1. Summary of geotechnical properties of sediments from the study area

| | Minimum | Maximum | Average | Standard deviation |
|--|---------|---------|---------|--------------------|
| Water content (%) | 308 | 504 | 399 | 52 |
| Specific gravity | 1.81 | 2.43 | 2.19 | 0.18 |
| Porosity (%) | 85.9 | 92.4 | 89.6 | 1.36 |
| Wet bulk density (g cm ⁻³) | 1.11 | 1.20 | 1.15 | 0.02 |
| Void ratio | 6.07 | 12.13 | 8.9 | 1.3 |
| Shear strength (kPa) | 2.15 | 14.72 | 7.16 | 2.91 |
| Sand (%) | 0.09 | 9.8 | 1.7 | 1.64 |
| Silt (%) | 34.84 | 71 | 45.7 | 8.1 |
| Clay (%) | 25.65 | 64.58 | 52.42 | 9.0 |
| Smectite (%) | 2.0 | 15.3 | 6.74 | 2.62 |
| Illite (%) | 34.3 | 63.8 | 51.5 | 6.2 |
| Kaolinite (%) | 10.4 | 26.9 | 18.92 | 3.3 |
| Chlorite (%) | 14.88 | 32.13 | 23.1 | 3.9 |

Table 2. Correlation matrix ($n = 60$, conf. level = 99%)

| | W | G | Sand | Silt | Clay | Sm | I | K | C | ss |
|------|---------------|-------|---------------|---------------|---------------|--------|---------------|---------------|-------|----|
| W | 1 | | | | | | | | | |
| G | -0.096 | 1 | | | | | | | | |
| Sand | -0.464 | 0.074 | 1 | | | | | | | |
| Silt | -0.447 | -0.04 | 0.469 | 1 | | | | | | |
| Clay | 0.490 | 0.016 | -0.590 | -0.988 | 1 | | | | | |
| Sm | 0.004 | -0.25 | 0.055 | -0.067 | 0.039 | 1 | | | | |
| I | -0.218 | 0.239 | 0.206 | 0.366 | -0.385 | -0.172 | 1 | | | |
| K | 0.224 | -0.17 | -0.26 | -0.436 | 0.459 | -0.13 | -0.817 | 1 | | |
| C | 0.154 | -0.07 | -0.15 | -0.173 | 0.202 | -0.292 | -0.787 | 0.539 | 1 | |
| ss | -0.635 | 0.212 | 0.288 | 0.338 | -0.375 | 0.196 | 0.256 | -0.355 | -0.24 | 1 |

W, Water content; G, Specific gravity; Sm, Smectite, I, Illite; K, Kaolinite; C, Chlorite and ss, Shear strength. Bold numbers show significant correlations.

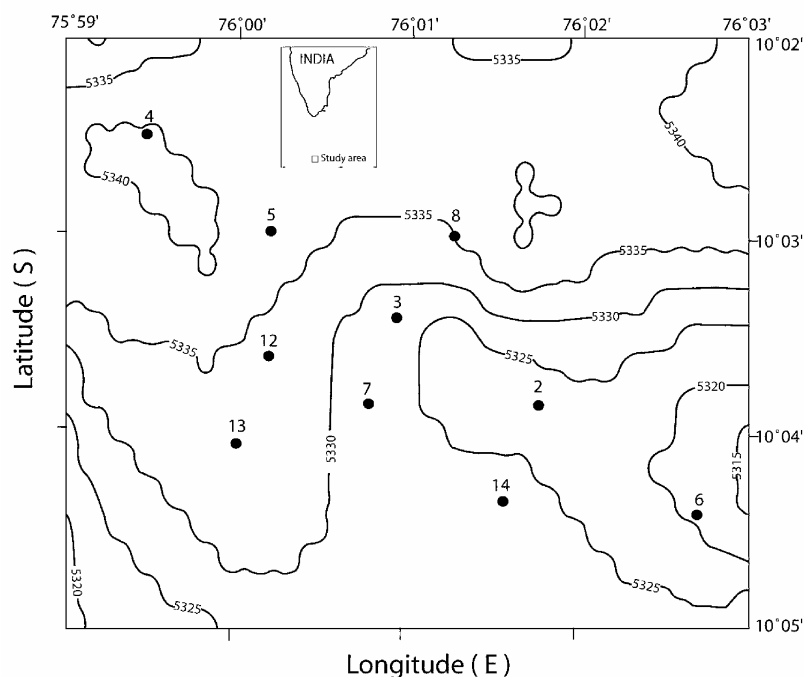


Figure 1. Box-core locations (solid circles) in the study area with bathymetric contours (in m).

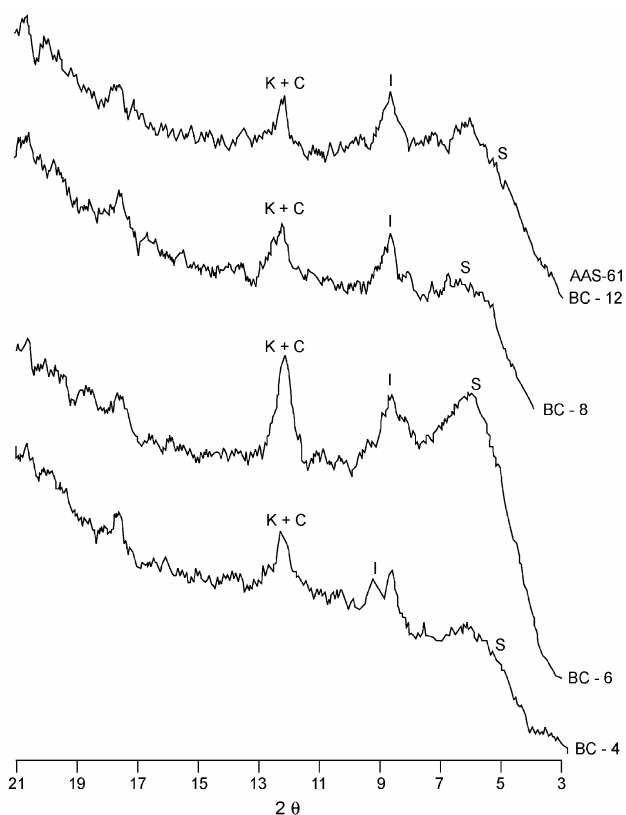


Figure 2. Typical X-ray diffractograms of <2 μm glycolated samples. S, Smectite; I, Illite; K, Kaolinite and C, Chlorite.

A strong negative relationship of clay with silt ($r = -0.988$) supports that clay is dominant in the CIB sediments. In most of the samples illite is dominating and is of detrital origin. The shear strength is positively correlated to silt ($r = 0.338$) and inversely to clay ($r = -0.375$), indicating that it is more controlled by clay than silt. The small amount of kaolinite (av 18.92%) present in the samples shows negative effect on shear strength. Strong relationship of water content with porosity ($r = 0.799$) and wet bulk density ($r = -0.825$) reported for other ocean sediments¹⁵ was observed in these sediments. Since earlier studies¹¹ have shown that the siliceous sediments from the CIB are highly plastic, their shear strength is expected to be higher during *in situ* measurements than on-board measurements.

High water content (308–504%) of the CIB sediments is related to clay and silt contents than any clay mineral composition. Shear strength of these cohesive sediments increases gradually with core depth and is related negatively with water content, clay per cent and kaolinite content. The positive relationship between silt content and shear strength could be due to flocculating characteristics of illite-rich silt grains. High void ratio and porosity indicate poor sorting of fine particles leading to isotropic fabric and high water content.

1. Radziejewska, T. and Modlitba, I., In Proceedings of the Third ISOPE-Ocean Mining Symposium, Goa, 1999, pp. 126–130.
2. Rowe, G. T., In *Deep-Sea Sediments: Physical and Mechanical Properties* (ed. Inderbitzen, A. L.), Plenum Press, New York, 1974, pp. 381–400.
3. Banakar, V. K., Gupta, S. M. and Padmavati, V. K., *Mar. Geol.*, 1991, **96**, 167–173.
4. Sharma, R., Nath, B. N., Valsangkar, A. B., Khadge, N. H., Gupta, S. M. and Parthiban, G., In Proceedings of International Symposium on Environmental Studies for Deep-Sea Mining, Tokyo, 20–21 November 1997, pp. 83–90.
5. Noorany, I., *J. Geotech. Eng., ASCE*, 1984, **110**, 539–543.
6. American Society for Testing and Materials, *Annual Book of ASTM Standards, 04.08 Soil and Rocks (I): D420–D4914*, ASTM, Philadelphia, 1995, p. 981.
7. Bennett, R. H. and Lambert, D. N., *Mar. Geol.*, 1971, **11**, 201–207.
8. Folk, R. L., *Petrology of Sedimentary Rocks*, Hemphill's, Texas, 1968, p. 170.

9. Biscaye, P. E., *Geol. Soc. Am. Bull.*, 1965, **76**, 803–832.
10. Bowles, F. A., Bryant, W. R. and Wallin, C., *J. Sediment. Petrol.*, 1969, **39**, 1546–1551.
11. Khadge, N. H., In Proceedings of the Third ISOPE-Ocean Mining Symposium, Goa, 1999, 138–144.
12. Keller, G. H., In *Deep-Sea Sediments: Physical and Mechanical Properties* (ed. Inderbitzen, A. L.), Plenum Press, New York, 1974, pp. 77–100.
13. Bennett, R. H., Fischer, K. M., Lavoie, D. L., Bryant, W. R. and Rezek, R., *Mar. Geol.*, 1989, **89**, 127–152.
14. Debrabant, P., Fagel, N., Chamley, H., Bout, V. and Culet, J. P., *Palaeogeogr.*

- Palaeoclimatol. Palaeoecol.*, 1993, **103**, 117–131.
15. Richards, A. F., Investigation of deep sea sediments cores. II-Mass physical properties. US Navy Hydrographic Office Technical Report 106, 1962, p. 146.

ACKNOWLEDGEMENTS. We thank the Director, National Institute of Oceanography, Goa for permission to publish the data; the crew and participants of *AA Sidorenko-61* for help during sampling; and Mr G. Prabhu for help during X-ray diffraction analysis. Financial support was received from the Ministry of Earth Sciences, Govt of India. Thanks are also due to the anonymous referees whose com-

ments helped improve the manuscript. This is NIO contribution no. 4360.

Received 25 May 2007; revised accepted 2 April 2008

N. H. KHADGE*
A. B. VALSANGKAR

*National Institute of Oceanography,
Dona Paula,
Goa 403 004, India*
*For correspondence.
e-mail: khadge@nio.org

Occurrence of sandstone-type uranium mineralization in the Umthongkut area, Mahadek Basin, West Khasi Hills District, Meghalaya, India

Exploration of the Upper Cretaceous Mahadek sediments by the Atomic Minerals Directorate for Exploration and Research (AMD) over the last four decades has established the country's two largest sandstone-type uranium deposits, viz. Domiasiat^{1–4} and Wahkyn⁵ in West Khasi Hills District, Meghalaya. Mahadek sediments are proximal sandy braided type deposited in fluvial environment⁴, which extends from the Jaintia Hills in the east to the Garo Hills in the west over a stretch of nearly 200 km. Significant uranium mineralization was located west of Umthongkut village (Figure 1) in part of T.S. No. 78K/15, about 205 km SW of Shillong, in the Mahadek sediments exposed along deep gorges and escarpment sections accessible only by forest foot track. This correspondence deals with the location, geology, preliminary petrological characters and genetic aspects of U-mineralization.

Geomorphologically, the area exhibits a highly dissected terrain with deep gorges, scanty plateau and sub-dendritic drainage pattern. Geologically, the area consists of Precambrian crystallines, Cretaceous fluvial Mahadek Formation and Tertiary marine Tura and Siju formations (Figure 1). Basement crystallines are represented by granite gneiss and migmatite, exposed to the west of Umthongkut nala and are unconformably overlain by the Upper Cretaceous Maha-

dek Formation that, in turn, is overlain by the Tura and Siju formations. The Mahadek Formation is predominantly arenaceous. On the basis of its colour, alteration, lithology, sedimentology, petrology and depositional characteristics it is divided into Lower and Upper sediments^{6–8}. The Lower Mahadek sediments are reduced, grey-coloured feldspathic-arenite and feldspathic-wacke, rich in carbonaceous matter (Figure 2), pyrite, resin and petrified wood. These are shallow-dipping (5–7° due southwest) beds forming an east-facing, north-south trending escarpment that is exposed persistently over a length of 1500 m with thickness varying from 5 to 60 m. The Upper Mahadek sediments are oxidized, purple-coloured, feldspathic-arenite and feldspathic-wacke. The Tura and Siju formations consist of arenaceous and calcareous components respectively, with thick seams of coal measuring up to 6 m.

The area has two sets of faults trending NNE–SSW and E–W. The fault pattern and disposition of rocks indicate that the NNE–SSW trending fault is younger. These faults have played a major role in exposing the basement crystallines and Lower Mahadek sediments, which are otherwise concealed under the Tertiary country. There has been differential movement due to the pivotal nature of these faults. As a consequence, the Tura Formation has come in direct contact

with the Lower Mahadek sediments in the southern part and with basement crystallines in northern and eastern parts.

In the Lower Mahadek sediments, sixteen uraniumiferous zones of varying dimensions and spread over an area of 1500 m × 300 m were recorded (Table 1). The dispositions of these zones vary from 1 to 15 m above the basement. Thickness of the mineralized zones in the middle and southern part of the area is more significant compared to the northern part, as evident from the uranium content, dimension of uranium anomalies and host-rock thickness. Cross-bedding, ripple marks and cut-and-fill structures are observed occasionally in the host rock, indicating it to be channel-fill sandstone. Physical assay ranges from 0.01 to 0.41% U₃O₈ (average 0.1% U₃O₈, *n* = 54) with spot values ranging from 0.7 to 9.98% U₃O₈ (*n* = 6). Sixty-one per cent of the samples shows disequilibrium in favour of the parent ranging from 15 to 250% (*n* = 36) and 36% in favour of the daughter, which ranges from 4 to 96% (*n* = 21); however, the two samples are in equilibrium.

Uranium mineralization is manifested as (a) U–C complex, (b) pitchblende, (c) coffinite and (d) U–Ti phases grading to brannerite. In addition, low concentration of uranium is associated with hydrated iron-oxide and clay. U–C complex occurs as thin streaks, layers, lumps and disper-